symmetry

MDPI

Article

Electronic Particle-Density Asymmetry in Doped Bilayer Graphene with Effective Fractional Dimensionality

Juan A. Lazzús * and L. Palma-Chilla

Departamento de Física, Universidad de La Serena, Casilla 554, La Serena 1700000, Chile
* Correspondence: jlazzus@userena.cl

Abstract

This work investigates how effective fractional dimensionality and substitutional doping jointly affect particle-density symmetry in AA-stacked bilayer graphene (BLG). The system consists of one pristine graphene layer and one doped layer, where 50% of the atomic sites are substituted. Doping is described within a tight-binding framework through a dimensionless parameter α (with $0 < \alpha < 1$), which uniformly reduces the intralayer hopping energy in the doped layer, while an effective fractional dimension $D > 2$ phenomenologically accounts for structural inhomogeneities such as ripples or corrugations. Analytical expressions for the energy spectrum and number of states are obtained, and the electronic asymmetry between layers is characterized by a symmetry parameter P. We find that substitutional doping breaks the particle-density symmetry of pristine BLG and strongly enhances the number of states near the Fermi level as α decreases, due to the accumulation of low-energy states in the doped layer. Departures from the ideal dimensionality $D = 2$ further amplify this enhancement. The combined effects of reduced α and increased D lead to a pronounced layer asymmetry, reflected in a nonzero P, while stronger interlayer coupling partially counteracts this imbalance. Results show that doping, effective fractional dimensionality, and interlayer coupling offer tunable control over the low-energy electronic properties of BLG.

Keywords: fractional dimensionality; bilayer graphene; electronic polarization; controlled doping

1. Introduction

In pristine conditions, graphene is a crystal of carbon atoms arranged in a honeycomb lattice within a strictly two-dimensional space [1,2]. However, experimental observations of corrugations, ripples, strain, and structural disorder suggest that the effective dimensionality of graphene can deviate from the ideal $D = 2$, giving rise to novel physical phenomena that can be interpreted in terms of a fractional dimension [3].

According to the Mermin–Wagner theorem, there should be no long-range order in two-dimensional systems at finite temperature. Instead, the system is expected to develop dislocations under any nonzero thermal conditions [4,5]. Thus, an important issue is the role of these defects in the thermodynamic stability of two-dimensional crystals, since geometrical deformations, such as thermally induced ripples, modify the available electronic states. Flores and Palma-Chilla demonstrated that such ripples lead to an effective spatial dimension of $D \approx 2.18$ at room temperature in a pristine graphene sheet, altering thermodynamic quantities such as entropy, internal energy, and specific heat. Moreover, this fractional dimension increases as temperature rises [3]. Therefore, it is relevant to

Check for updates

Academic Editor: Sergei Odintsov

Received: 13 January 2026
Revised: 6 February 2026
Accepted: 17 February 2026
Published: 23 February 2026

Copyright: © 2026 by the authors. Licensee MDPI, Basel, Switzerland. This article is an open access article distributed under the terms and conditions of the Creative Commons Attribution (CC BY) license.

extend these studies to doped and multilayer graphene systems, where additional factors such as doping, interlayer coupling, and stacking order may further modify the effective dimensionality and, consequently, the thermodynamic responses of the system, including variations in carrier distribution, the total number of states, the density of states, band asymmetry, and thermoelectric properties [6–9].

This study explores the impact of effective fractional dimensionality and doping on the electronic layer symmetry of a bilayer graphene composed of one pristine layer and one doped layer (in which 50% of the atomic sites are substituted). Our approach investigates how the interplay between effective fractional dimension and doping modifies the number of states, thereby providing new insights into the electronic structure of doped bilayer graphene systems. Unlike earlier approaches that associated fractional dimensionality with a real-space geometric modification [3], here it is introduced as an effective spectral parameter within the dispersion and state-counting formalism, without altering the lattice geometry. This spectral formulation enables an analytical, layer-resolved description of particle populations and symmetry breaking that is not accessible in previous fractional-dimensional frameworks. In bilayer graphene, electronic layer symmetry refers to the equivalence of the two atomic layers in terms of charge distribution and electronic wavefunction overlap [2]. In the pristine case, both layers contribute equally to the total electronic population, resulting in a symmetric interlayer coupling that preserves inversion symmetry. However, when one layer is doped, this balance should be disrupted due to charge redistribution between layers and the emergence of an electronic polarization [10]. In this work, the degree of asymmetry is quantified by a symmetry parameter P, which serves as an internal order parameter reflecting how doping and effective fractional dimensionality break the particle-density symmetry. To the best of our knowledge, no previous studies have quantified how these two mechanisms interact or how their interplay could improve the design of bilayer systems with tunable electronic properties.

2. Bilayer Doped Graphene

To study the combined effects of effective fractional dimensionality and substitutional doping on the electronic properties of bilayer graphene (BLG), we employ a simple model consistent with the scope of this work. We consider an AA-stacked BLG composed of one pristine layer, with all sites occupied by carbon atoms, and one doped layer, where 50% of the sites are substituted, and assuming that the intralayer hopping energies are uniformly reduced by a factor α, which effectively parameterizes the average weakening of electronic coupling induced by substitutional dopants [7]. Figure 1a shows a schematic representation of the BLG system used. Thus, this model can be represented by a 4×4 Hamiltonian in the energy basis, including the interlayer coupling:

$$H\left(\vec{k}\right) = \begin{pmatrix} E_0\left(\vec{k}\right) & \Delta & 0 & 0 \\ \Delta & \alpha E_0\left(\vec{k}\right) & 0 & 0 \\ 0 & 0 & -E_0\left(\vec{k}\right) & \Delta \\ 0 & 0 & \Delta & -\alpha E_0\left(\vec{k}\right) \end{pmatrix}, \quad (1)$$

where $E_0\left(\vec{k}\right) = \hbar v_F \left|\vec{k}\right|$ represents the energy of pristine graphene layer, v_F is the Fermi velocity and $\vec{k} = \left(k_x, k_y\right)$ is the wave vector. The parameter Δ denotes the interlayer hopping between the pristine and doped layers and is treated as k-independent

for our purposes. Altogether, Equation (1) captures the electron–hole symmetry of the doped bilayer.

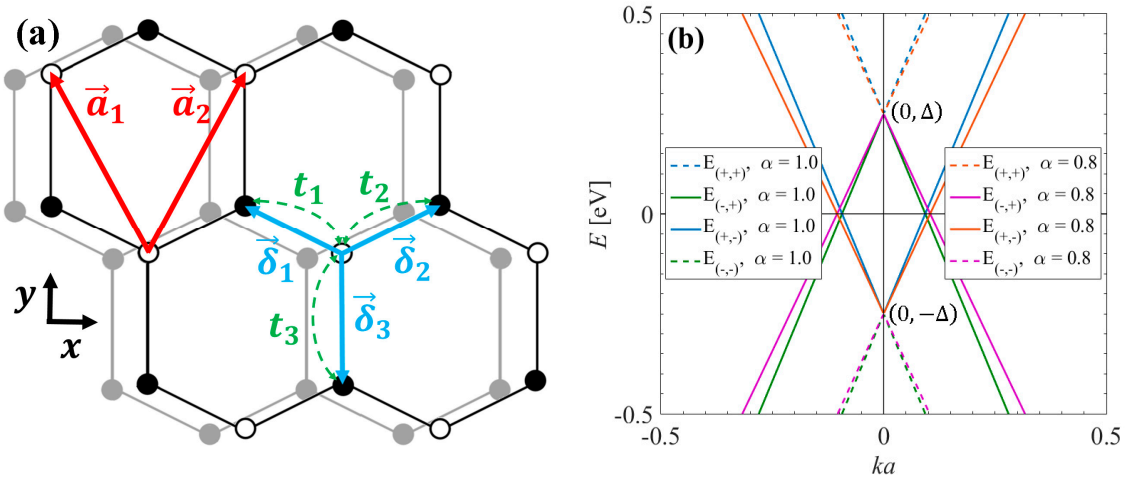


Figure 1. (**a**) Schematic of the bilayer graphene honeycomb lattice showing the primitive vectors $\vec{a}_1$ and $\vec{a}_2$, the lattice vectors $\vec{\delta}_1$, $\vec{\delta}_2$, and $\vec{\delta}_3$, and the hopping parameters t_1, t_2, and t_3. The gray layer represents pristine graphene composed of carbon atoms, while the layer with white and black atoms corresponds to the doped graphene sheet with 50% carbon and 50% dopant atoms. (**b**) Energy band spectra of bilayer graphene obtained from Equation (2), where all branches are symmetric with respect to $E = 0$. Here we contrast the pristine BLG case ($\alpha = 1$) with the doped case ($\alpha = 0.8$), showing the inner branches with solid lines and the outer branches with dashed lines.

In the layers of this system, we use the standard tight-binding method on the honeycomb lattice geometry [1,2]. Considering E_0 as the energy spectrum of the pristine sheet, with intralayer hopping $t_0 \approx 2.7$ eV, the doped layer is modeled by uniformly scaling to αE_0. This implies modified hoppings, with $\alpha = t_i/t_0$ (for $i = 1, 2, 3$) representing the reduced hopping energy caused by the altered electronic overlap between the carbon and dopant atoms (see Figure 1a). This formalism assumes that, for small values of $\vec{k}$, all hopping processes involving a dopant atom are uniformly scaled by the same factor α, thus maintaining translational invariance in the effective tight-binding Hamiltonian. Thus, for typical n- or p-dopants, $0 < \alpha < 1$, this scaling preserves the overall topology of the pristine spectrum [7]. Note that the parameter α is specific to our model and can, in principle, be obtained from DFT studies [11,12]. However, when intralayer hopping data are not available for a specific dopant, an alternative and practical method to estimate this parameter was proposed in [7].

Solving the eigenvalue problem for Equation (1) yields the energy spectrum:

$$E_{(s_1,s_2)} = \frac{s_1}{2}\left[(1+\alpha)E_0 + s_2\sqrt{(1-\alpha)^2E_0^2 + 4\Delta^2}\right], \tag{2}$$

where $s_1 = \pm 1$ labels the conduction $(+)$ and valence $(-)$ branches, while $s_2 = \pm 1$ distinguishes the inner and outer bands within each pair. Accordingly, the full spectrum consists of four energy branches $E = \left\{E_{(+,+)}, E_{(-,+)}, E_{(+,-)}, E_{(-,-)}\right\}$, which appear as symmetric pairs about $E = 0$ (see, Figure 1b). It is worth noting that, for $\Delta = 0$, the spectrum recovers the expected energy branches $\{E_0, \alpha E_0, -E_0, -\alpha E_0\}$. For $\Delta \neq 0$, a symmetric overlap between the inner conduction and valence branches emerges around $E = 0$. In addition, the factor α describes the modification of the energy parameter in the doped layer. If $\alpha \neq 1$, $0 < \alpha < 1$, asymmetry arises between the two layers, and the energy bands flatten due to the reduced intralayer hopping in the doped layer. For

$\alpha = 1$ (symmetric layers), the system reduces to the pristine BLG case. Figure 1b shows the complete spectrum of the system described in Equation (2), as well as the effects of the model parameters on it.

3. Number of States

We focus the analysis on the low-energy region $-\Delta < E < \Delta$, corresponding to the inner energy branches $E = \left\{E_{(-,+)}, E_{(+,-)}\right\}$ (see, Figure 1b). Within this interval, the band structure can be consistently reduced to a low-energy subspace, allowing analytical expressions for both the cumulative number of states and the particle number.

Since the energy of the pristine layer can be expressed in terms of the energy of the doped layer (inverted Equation (2)), this allows us to define a hyperspherical surface in $\vec{k}$-space with radius $r = \left|\vec{k}\right|$ [6]. This mapping enables a direct characterization of the spectrum and the definition of the number of states per particle as:

$$\begin{gathered} N_{(s_1,s_2)}(E) = \frac{\pi^{D/2}}{\Gamma\left(\frac{D}{2}+1\right)}\left(\frac{a}{2\alpha\hbar v_F}\right)^D [s_1(1+\alpha)E - s_2\xi]^D, \\ \xi(E) = \sqrt{(1-\alpha)^2E^2 + 4\alpha\Delta^2}, \end{gathered} \tag{3}$$

where $s_1 = \pm 1$ labels the conduction and valence branches, respectively, while $s_2 = \pm 1$ distinguishes the inner and outer bands within each pair, where the complete spectrum consists of four symmetric hyperspherical branches $N(E) = \left\{N_{(+,+)}, N_{(+,-)}, N_{(-,+)}, N_{(-,-)}\right\}$. In addition, a is a characteristic length scale associated with the unit cell of the graphene lattice ($a \sim 2.46$ Å), and $\Gamma(x)$ is the Gamma function. Although the formal expression includes all four branches, the number of states is physically meaningful only for the inner bands in the interval $E \in [-\Delta, \Delta]$, since only they fall within the low-energy regime where the mapping $E \leftrightarrow E_0$ is valid and the hyperspherical radius is well defined. Within this interval, there can exist two specific intersection points that map to the same energy $E = 0$ in each branch, located at $E_0 = \Delta/\sqrt{\alpha}$ (that is, $k = \Delta/\hbar v_F\sqrt{\alpha}$ for both $E_{(-,+)}$ and $E_{(+,-)}$ (see, Figure 1b). Consequently, the cumulative number of states at zero energy scales as $N(E=0) \sim \left(\Delta/\sqrt{\alpha}\right)^D$. As a result, the total number of states is given solely by the contribution of the inner symmetric pair, $N(E) = N_{(-,+)} + N_{(+,-)}$. Moreover, the parameter D represents the effective dimensionality of the system. Mathematically, the number of states with energy less than E is proportional to the volume of a D-dimensional hypersphere of radius $r(E)$, given by $V(r, D) = \pi^{D/2}r^D/\Gamma(D/2+1)$. In the case of pristine graphene, $D = 2$, reflecting the two-dimensional nature of the lattice, so that the number of states scales with the area of a circle in $k_x - k_y$ space. As mentioned in Section 1, under realistic conditions graphene is not perfectly flat but exhibits ripples, corrugations, and lattice deformations that alter the electronic spectrum and the number of states [13–16]. Thus, these effects can be phenomenologically encoded through an effective fractional dimensionality, which parametrizes deviations from the ideal two-dimensional state counting in the k-space [6]. Since the Gamma function $\Gamma(D/2+1)$ allows a smooth extension of D to non-integer values, physically the hypersphere defined for fractional D does not represent a classical geometry, but rather an equal-energy surface in a state space with an effective continuous dimensionality that quantifies the altered number of states induced by spatial inhomogeneities. Treating D as an effective fractional dimension makes this parameter crucial for connecting structural disorder with the number of electronic states. In this framework, D is not a real geometric dimension but a spectral phenomenological parameter that incorporates experimentally observed ripples and corrugations into the state-counting description; values around $D \approx 2.2$ are consistent with prior reports for thermally rippled graphene [3].

Note that Equation (3) is defined per particle, i.e., per unit cell of effective D-dimensional volume a^D, obtaining the total number of states requires multiplying by the number of effective cells that compose the system. For a system of linear size L, this introduces a factor $(L/a)^D$. Therefore,

$$n(E) = \left(\frac{L}{a}\right)^D N_{(s_1,s_2)}(E), \tag{4}$$

converts the per-particle expression into the total number of states in a system of finite size.

Subsequently, we convert $n(E)$ into its reduced form $n(\varepsilon)$ by introducing the natural energy scale of the system, $\alpha\hbar v_F/a$, and we define the reduced variables $\varepsilon = E/(\alpha\hbar v_F/a)$ and $\widetilde{\Delta} = \Delta/(\alpha\hbar v_F/a)$. In this way, the number of states is expressed solely in terms of the intrinsic parameters of our model:

$$\widetilde{N}_{(s_1,s_2)}(\varepsilon) = \frac{\pi^{D/2}}{\Gamma\left(\frac{D}{2}+1\right)}\left(\frac{1}{2a}\right)^D \left[s_1(1+\alpha)\varepsilon - s_2\widetilde{\xi}\left(\varepsilon,\widetilde{\Delta}\right)\right]^D, \tag{5}$$

where the auxiliary quantity $\widetilde{\xi}\left(\varepsilon,\widetilde{\Delta}\right)$ is the adimensional counterpart of $\xi(E,\Delta)$. With this, the relevant interval for our study becomes $-\widetilde{\Delta} < \varepsilon < \widetilde{\Delta}$.

In order to establish a direct correspondence between the cumulative number of states and the total number of particles, the zero-temperature limit ($T = 0$ K) is adopted. In this limit, the total particle number is exactly given by the cumulative number of states evaluated at the Fermi energy, provided that all relevant degeneracies are properly accounted for [17,18].

Figure 2 shows the behavior of $n(\varepsilon)$ in the interval $-\widetilde{\Delta} < \varepsilon < \widetilde{\Delta}$. This figure compares the effects of typical dopants such as N or B atoms, with $\alpha \approx 0.8$ and 0.9 in one layer of the BLG [7], against the pristine BLG case ($\alpha = 1$), using effective fractional dimensionality values $D = 2$ and $D = 2.2$. Panel (a) displays the asymmetric behavior of $n(\varepsilon)$ (with respect to $\varepsilon \neq 0$) for $\Delta = 0.5$ eV ($\widetilde{\Delta} = 0.19$), also under small variations in the effective fractional dimension. Moreover, panel (b) shows the effect of substitutional doping on $n(\varepsilon)$ for doped BLG (at $\Delta = 0.5$ eV and $D = 2$), comparing $\alpha = 1$ with $\alpha = 0.8$ and 0.9. Finally, panel (c) presents a similar analysis to panel (b) but using $D = 2.2$. In all panels, for $\alpha = 1$ case, at $D = 2$, the curves reproduce the expected linear behavior of pristine BLG with AA-stacking in the low-energy regime, reflecting the ideal dispersion case. When substitutional doping is introduced in one layer ($0 < \alpha < 1$), $n(\varepsilon)$ shows a significantly enhanced contribution at low energies compared to $\alpha = 1$. This effect is a direct consequence of the reduced hopping energies in the doped layer, which increases the availability of states close to the Fermi level. In addition, since our formalism incorporates the dimensionality parameter D, we note that small deviations from the ideal value $D = 2$ shifts $n(\varepsilon)$ to higher values. Therefore, increasing the effective fractional dimension enhances the number of available states in the low-energy regime, as higher D values increase the concentration of states per energy.

On the other hand, comparing the effects of heavy dopant atoms in one layer, e.g., $\alpha = 0.8$, versus the pristine case $\alpha = 1$, by using fractional dimension values $D = 2$ and $D = 2.2$. As observed, strong doping (α significantly smaller than 1) amplifies this trend. In fact, for $\alpha = 0.8$ and $D = 2.2$, an additional enhancement arises in the low-energy values of $n(\varepsilon)$, showing that reduced α can reinforce the increase induced by higher effective dimensionality.

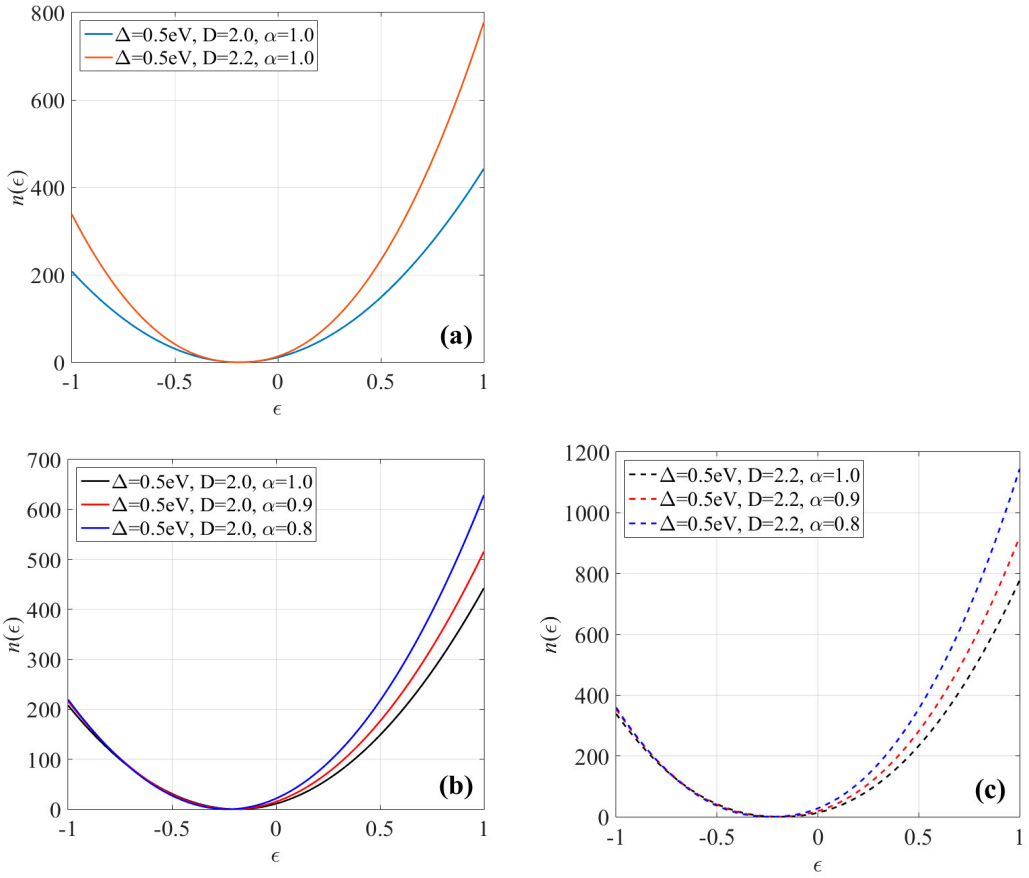


Figure 2. Cumulative number of states $n(\varepsilon)$ in the interval $-\widetilde{\Delta} < \varepsilon < \widetilde{\Delta}$. Panel (**a**) shows pristine BLG ($\alpha = 1$), illustrating the transition from a symmetric profile at $\widetilde{\Delta} = 0$ to an asymmetric one at finite $\widetilde{\Delta}$ (using $\Delta = 0.5$ eV), for $D = 2$ and $D = 2.2$. Panels (**b**,**c**) present doped BLG, comparing $\alpha = 1$ with $\alpha = 0.9$ and $\alpha = 0.8$ at finite $\widetilde{\Delta}$ (with $\Delta = 0.5$ eV), for $D = 2$ and $D = 2.2$, respectively, highlighting the enhancement and asymmetry of $\rho(\varepsilon)$ induced by doping and effective fractional dimensionality. All figures were constructed using: $\hbar = 6.58 \times 10^{-16}$ [eV·s]; $v_F = 10^6$ [m/s]; $\Delta = 0.5$ [eV]; $a = 2.46 \times 10^{-10}$ [m]; and $L = 10a$ [m].

The asymmetries observed in the density of states within the interval $-\widetilde{\Delta} < \varepsilon < \widetilde{\Delta}$ reveal that the availability of electronic states is no longer evenly distributed around the Fermi level when doping and fractional dimensionality are present. To quantify this effect more rigorously, we introduce a symmetry parameter, which provides a direct and quantitative measure of the degree of electronic asymmetry induced by doping.

4. Particle-Density Symmetry

Our doped bilayer system can be viewed as a transition from a symmetric regime ($\alpha = 1$, $D = 2$) to an asymmetric regime ($0 < \alpha < 1$, $D > 2$), featuring a breaking of layer equivalence induced by α and a loss of spatial homogeneity associated with the effective fractional dimension D. Both effects define a new regime of reduced symmetry, which is manifested in the electronic spectrum (see Figure 1b) and in the number of states of our system (see Figure 2).

To quantify the particle-density symmetry breaking induced by these parameters, we consider the eigenvector associated with Equation (1). As mentioned in Section 1, the spectrum of the system is symmetric with respect to $E = 0$; therefore, we only consider the

eigenvector corresponding to the conduction-band block of the Hamiltonian, which can be expressed as a two-component spinor:

$$\vec{C}_{(s_1,s_2)} = \begin{pmatrix} c_1\left(E_{(s_1,s_2)}\right) \\ c_2\left(E_{(s_1,s_2)}\right) \end{pmatrix} = \begin{pmatrix} 1 \\ \frac{E_{(s_1,s_2)}-E_0}{\Delta} \end{pmatrix}, \tag{6}$$

where c_1 is the amplitude on the pristine layer, and c_2 the amplitude on the doped layer whose squared moduli, $|c_1|^2$ and $|c_2|^2$, represent the weighting factors of quantum hybridization between the two graphene layers, indicating how much each layer contributes to the energy eigenstate $E_\pm$ [2]. Note that the eigenvector must satisfy the normalization condition $|c_1|^2 + |c_2|^2 = 1$. In addition, these weights depend on the energy separation $E_{(s_1,s_2)} - E_0$ and the interlayer coupling Δ, revealing how the interlayer quantum mixing varies with energy:

$$\begin{aligned} \left|c_1\left(E_{(s_1,s_2)}\right)\right|^2 &= \frac{\Delta^2}{\Delta^2+\left(E_{(s_1,s_2)}-E_0\right)^2}, \\ \left|c_2\left(E_{(s_1,s_2)}\right)\right|^2 &= \frac{\left(E_{(s_1,s_2)}-E_0\right)^2}{\Delta^2+\left(E_{(s_1,s_2)}-E_0\right)^2}. \end{aligned} \tag{7}$$

These equations show that for $E_{(s_1,s_2)} \to E_0$, the electron is equally distributed between layers (symmetric regime), whereas at higher or lower energies, one layer becomes dominant (asymmetric regime).

Taking the energy solutions for the system branches from Equation (2) and subtracting the pristine energy, the energy difference is obtained as $E_{(s_1,s_2)} - E_0 = \frac{1}{2}((\alpha-1)E_0 + s_2\zeta)$, with $\zeta(E_0) = \sqrt{(1-\alpha)^2E_0^2 + 4\Delta^2}$. Replacing this expression in Equation (8) and simplifying, we then introduce the normalized variables ε_0, $\widetilde{\Delta}$, and $\widetilde{\zeta}$ (see Equation (5)), which allow us to express all quantities in dimensionless form:

$$\begin{aligned} \left|c_1\left(\varepsilon_{(s_1,s_2)}\right)\right|^2 &= \frac{4\widetilde{\Delta}^2}{4\widetilde{\Delta}^2+\left((\alpha-1)\varepsilon_0+s_2\widetilde{\zeta}\right)^2}, \\ \left|c_2\left(\varepsilon_{(s_1,s_2)}\right)\right|^2 &= \frac{\left((\alpha-1)\varepsilon_0+s_2\widetilde{\zeta}\right)^2}{4\widetilde{\Delta}^2+\left((\alpha-1)\varepsilon_0+s_2\widetilde{\zeta}\right)^2}, \end{aligned} \tag{8}$$

where the dependence on doping (α) becomes explicit. If $\alpha = 1$ and $\Delta \neq 0$, the formulas return the expected symmetric weights; if $\Delta \to 0$, the weighting factors approach 0/1, corresponding to complete layer localization. When $0 < \alpha < 1$, the balance between both components is progressively distorted: the weights become energy dependent in an asymmetric way within the interval $-\widetilde{\Delta} < \varepsilon < \widetilde{\Delta}$, producing a preferential occupation of one layer over the other. This electronic symmetry/asymmetry of the system can be quantified using a symmetry parameter defined as:

$$P\left(\varepsilon_{(s_1,s_2)}\right) = \left(|c_1|^2 - |c_2|^2\right)n_{(s_1,s_2)}(\varepsilon) = \frac{4\widetilde{\Delta}^2 - \left((\alpha-1)\varepsilon_0 + s_2\widetilde{\zeta}\right)^2}{4\widetilde{\Delta}^2 + \left((\alpha-1)\varepsilon_0 + s_2\widetilde{\zeta}\right)^2}n_{(s_1,s_2)}(\varepsilon), \tag{9}$$

where P is an internal electronic order parameter that measures the occupancy asymmetry between the two layers of the system. The difference $|c_1|^2 - |c_2|^2$ quantifies the imbalance in the probability of finding the electron in each layer, so that vanishing values correspond to a symmetric regime ($P = 0$), while finite values indicate a preferential localization induced by doping or by the interlayer coupling. By multiplying this difference by the number of available states $n_{(s_1,s_2)}(\varepsilon)$, this parameter accounts not only for the asymmetry of an individual state but also for how many states effectively contribute to such asymmetry at a

given energy. In this sense, $P(\varepsilon)$ provides a clear signature of particle-density symmetry breaking between layers in doped bilayer graphene, and can be physically interpreted as an electronic layer polarization associated with interlayer charge redistribution, serving as a theoretical proxy for measurable charge imbalance or electrostatic potential differences.

Figure 3 quantifies the imbalance of electronic occupation between the two layers of the bilayer graphene system. Panel (a) shows the combined effects of doping α and effective fractional dimension D on the particle-density asymmetry at a fixed interlayer coupling. When the system is pristine ($\alpha = 1$, $D = 2$), the particle density is perfectly balanced, resulting in a symmetric electron distribution between the two layers. In this case, $P(\varepsilon) = 0$ over the entire energy range, and the corresponding curve remains centered around zero, indicating equal contributions from both layers. In contrast, for doped configurations ($\alpha = 0.9$ and 0.8, at $D = 2$ and 2.2), the particle density becomes asymmetric, leading to $P(\varepsilon) \neq 0$. This nonzero value of P represents an electronic layer polarization directly associated with interlayer charge imbalance. This asymmetry reflects a preferential localization of electronic states in the doped layer, shifting P toward negative values. The use of 50% substitution corresponds to a symmetric, analytically tractable limit within an effective-medium description, where doping is treated as a uniform hopping renormalization that captures the mean spectral effect without resolving local disorder. Panel (b) illustrates the competition between the interlayer coupling, which tends to restore layer symmetry, and the energy imbalance introduced by doping, which favors asymmetry, in a BLG system with spatial inhomogeneities ($D = 2.2$). As the interlayer hopping increases, the magnitude of $P(\varepsilon)$ is reduced, indicating smaller deviations from symmetry, while the overall qualitative behavior is preserved. Although the calculation is performed for AA stacking, used here as a minimal platform, the same qualitative symmetry-breaking mechanism is expected to persist in AB-stacked bilayers with quantitative differences due to their more complex dispersion [19,20]. These results show that interlayer coupling can counteract the effects of doping on the electronic asymmetry of the system.

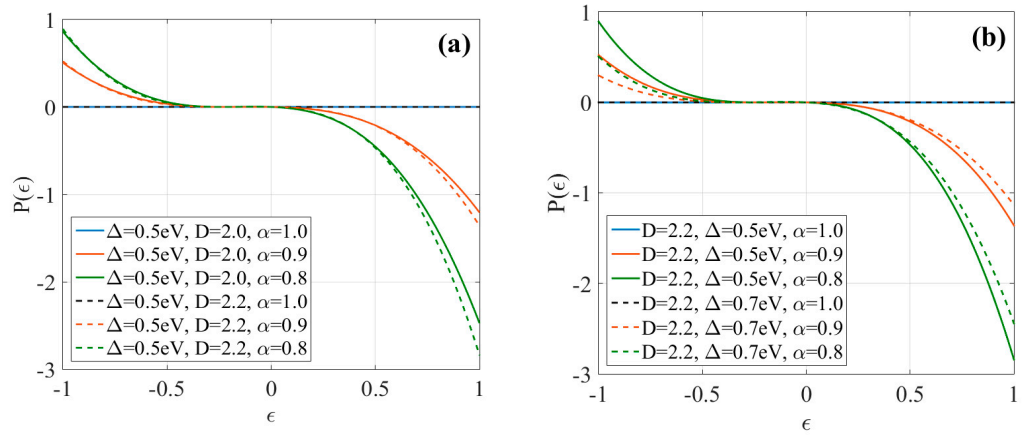


Figure 3. Particle-density asymmetry in doped BLG. Panel (**a**) shows the effects of α and D at fixed interlayer coupling. In the pristine case ($\alpha = 1$, $D = 2$), the electronic occupation is symmetric between layers and $P = 0$ over the full energy range. Doped systems ($\alpha = 0.9, 0.8$; $D = 2, 2.2$) exhibit a finite polarization, indicating preferential localization of electronic states in the doped layer. Panel (**b**) shows, for an inhomogeneous system ($D = 2.2$), the competition between interlayer coupling and doping: increasing the interlayer hopping reduces the magnitude of P, restoring layer symmetry. Both figures were constructed using: $\hbar = 6.58 \times 10^{-16}$ [eV·s]; $v_F = 10^6$ [m/s]; $a = 2.46 \times 10^{-10}$ [m]; and $L = 10a$ [m].

5. Conclusions

This work demonstrates that substitutional doping in a single layer of bilayer graphene produces profound and controllable modifications in its low-energy electronic properties. The density of states is strongly affected by both the reduction in the intralayer hopping parameter ($0 < \alpha < 1$) and by deviations from the ideal effective fractional dimensionality ($D = 2$). While pristine BLG exhibits the expected symmetric and linear low-energy behavior, doping enhances the density of states near the Fermi level by reducing the effective hopping in the doped layer, thereby increasing the availability of low-energy electronic states. This enhancement is further amplified when the system is described by an effective fractional dimensionality ($D > 2$), indicating that phenomenologically the spatial inhomogeneities or structural disorder can reinforce the electronic effects induced by dopants.

Furthermore, the combined analysis of the number of states and the polarization parameter reveals that doping breaks the particle-density symmetry between layers, leading to an energy-dependent imbalance in electronic occupation. This asymmetry increases with stronger doping (smaller α) and higher effective dimensionality, resulting in a preferential localization of electronic states in the doped layer. However, the interlayer coupling plays a counterbalancing role: increasing the interlayer hopping tends to suppress the polarization and partially restore layer symmetry, even in doped and inhomogeneous systems. Overall, these results show that the interplay between doping strength, effective dimensionality, and interlayer coupling provides a versatile mechanism to tune both the low-energy number of states and the electronic symmetry properties of bilayer graphene.

Author Contributions: Conceptualization, J.A.L. and L.P.-C.; methodology, J.A.L. and L.P.-C.; software, J.A.L.; validation, J.A.L. and L.P.-C.; formal analysis, J.A.L. and L.P.-C.; investigation, J.A.L. and L.P.-C.; writing—original draft preparation, J.A.L. and L.P.-C.; writing—review and editing, J.A.L. and L.P.-C. All authors have read and agreed to the published version of the manuscript.

Funding: This research was funded by DIDULS project PR2453857.

Data Availability Statement: The original contributions presented in the study are included in the article, further inquiries can be directed to the corresponding author.

Acknowledgments: The authors thank the support of the Direction of Research and Development of the University of La Serena (DIDULS) through project PR2453857, and the Department of Physics of the University of La Serena (DFULS) that enabled the preparation of this paper. Special thanks to J.C. Flores (UTA—Chile) for his comments, which greatly contributed to improving this paper.

Conflicts of Interest: The authors declare no conflicts of interest.

References

1. Castro Neto, A.H.; Guinea, F.; Peres, N.M.R.; Novoselov, K.S.; Geim, A.K. The electronic properties of graphene. *Rev. Mod. Phys.* **2009**, *81*, 109. [CrossRef]
2. McCann, E.; Koshino, M. The electronic properties of bilayer graphene. *Rep. Prog. Phys.* **2013**, *76*, 056503. [CrossRef]
3. Flores, J.C.; Palma-Chilla, L. Dirac fermions duality in graphene: Ripples and fractional dimensions as function of temperature. *Sci. Rep.* **2018**, *8*, 16250. [CrossRef] [PubMed]
4. Dartora, C.A. The breaking of Mermin-Wagner-Hohenberg's theorem for fractional systems. *Phys. Lett. A* **2024**, *496*, 129318. [CrossRef]
5. Fasolino, A.; Los, J.H.; Katsnelson, M.I. Intrinsic ripples in graphene. *Nat. Mater.* **2007**, *6*, 858–861. [CrossRef]
6. Flores, J.C.; Palma-Chilla, L.; Lazzús, J.A. Non-hermitian bilayer graphene with non-decaying states: Fractional dimension of electron-hole pairs. *Phys. B Condens. Matter* **2025**, *716*, 417719. [CrossRef]
7. Lazzús, J.A.; Palma-Chilla, L.; Flores, J.C. Electronic specific heat and thermal conductivity of bilayer graphene with pristine and parametrically doped layers: A study in the low-energy regime. *Phys. B Condens. Matter* **2026**, *720*, 417998. [CrossRef]

8. Palma-Chilla, L.; Lazzús, J.A.; Flores, J.C. Entropy and negative specific heat of doped graphene: Topological phase transitions and Nernst's Theorem revisited. *Entropy* **2024**, *26*, 771. [CrossRef] [PubMed]
9. Palma-Chilla, L.; Lazzús, J.A. Thermodynamic behavior of doped graphene: Impact of heavy dopant atoms. *Entropy* **2024**, *26*, 1093. [CrossRef] [PubMed]
10. Mousavi, H. Electronic properties of doped gapped graphene. *Phys. B Condens. Matter* **2013**, *414*, 78–82. [CrossRef]
11. Mann, S.; Rani, P.; Kumar, R.; Dubey, G.S.; Jindal, V.K. Thermodynamic properties of pure and doped (B, N) graphene. *RSC Adv.* **2016**, *6*, 12158–12168. [CrossRef]
12. Dai, X.S.; Shen, T.; Liu, H.C. DFT study on electronic and optical properties of graphene modified by phosphorus. *Mater. Res. Express* **2019**, *6*, 085635. [CrossRef]
13. Thiemann, F.L.; Scalliet, C.; Müller, E.A.; Michaelides, A. Defects induce phase transition from dynamic to static rippling in graphene. *Proc. Natl. Acad. Sci. USA* **2025**, *122*, e2416932122. [CrossRef]
14. Kim, C.-E.; Lee, J.; Walsh, A.; Lordi, V.; Bahr, D.F. Role of ripples in altering the electronic and chemical properties of graphene. *J. Chem. Phys.* **2022**, *156*, 054708. [CrossRef]
15. Friedrich, M.; Stefanelli, U. Ripples in Graphene: A variational approach. *Commun. Math. Phys.* **2020**, *379*, 915–954. [CrossRef] [PubMed]
16. Yang, G.; Li, L.; Lee, W.B.; Ng, M.C. Structure of graphene and its disorders: A review. *Sci. Technol. Adv. Mater.* **2018**, *19*, 613–648. [CrossRef] [PubMed]
17. Kittel, C.; Kroemer, H. *Thermal Physics*, 2nd ed.; W. H. Freeman and Company: New York, NY, USA, 1980.
18. Ashcroft, N.W.; Mermin, N.D. *Solid State Physics*; Hancourt College Publishing: New York, NY, USA, 1976.
19. Rozhkov, A.V.; Sboychakov, A.O.; Rakhmanov, A.L.; Nori, F. Electronic properties of graphene-based bilayer systems. *Phys. Rep.* **2016**, *648*, 1–104. [CrossRef]
20. Apinyan, V.; Kopeć, T.K. Comparative study of the AA and AB bilayer graphene structures in the external electric and magnetic fields. *Phys. E Low-Dimens. Syst. Nanostruct.* **2023**, *150*, 115701. [CrossRef]

Disclaimer/Publisher's Note: The statements, opinions and data contained in all publications are solely those of the individual author(s) and contributor(s) and not of MDPI and/or the editor(s). MDPI and/or the editor(s) disclaim responsibility for any injury to people or property resulting from any ideas, methods, instructions or products referred to in the content.